Inorg. Chem. **2009**, *48*, 375−385

Ru(II) Complexes of New Tridentate Ligands: Unexpected High Yield of Sensitized $^1O_2$

Yao Liu,[†] Richard Hammitt,[‡] Daniel A. Lutterman,[†] Lauren E. Joyce,[†] Randolph P. Thummel,*[,‡] and Claudia Turro*[,†]

Department of Chemistry, The Ohio State University, Columbus, Ohio 43210, and Department of Chemistry, University of Houston, Houston, Texas 77204-5003

Received August 27, 2008

Ru(II) complexes possessing new tridentate ligands with extended π systems, pydppx (3-(pyrid-2′-yl)-11,12-dimethyl-dipyrido[3,2-*a*:2′,3′-*c*]phenazine) and pydppn (3-(pyrid-2′-yl)-4,5,9,16-tetraaza-dibenzo[*a*,*c*]naphthacene), were synthesized and characterized. The investigation of the photophysical properties of the series $[Ru(tpy)_n(L)_{2-n}]^{2+}$ (L = pydppx, pydppn, $n = 0-2$) reveals markedly different excited state behavior among the complexes. The Ru(II) complexes possessing the pydppx ligand are similar to the pydppz (3-(pyrid-2′-yl)dipyrido[3,2-*a*:2′,3′-*c*]phenazine) systems, with a lowest energy metal-to-ligand charge transfer excited state with lifetimes of 1−4 ns. In contrast, the lowest energy excited state in the $[Ru(tpy)_n(pydppn)_{2-n}]^{2+}$ ($n = 0$, 1) complexes is a ligand-centered $^3\pi\pi^*$ localized on the pydppn ligand with lifetimes of ∼20 μs. The $[Ru(tpy)_n(pydppn)_{2-n}]^{2+}$ ($n = 0$, 1) complexes are able to generate $^1O_2$ with ∼100% efficiency. Both $[Ru(tpy)(pydppn)]^{2+}$ and $[Ru(pydppn)_2]^{2+}$ bind to DNA, however, the former exhibits a ∼10-fold greater DNA binding constant than the latter. Efficient DNA photocleavage is observed for $[Ru(tpy)(pydppn)]^{2+}$, owing to its ability to photosensitize the production of $^1O_2$, which can mediate the reactivity. Such high quantum yields of $^1O_2$ photosensitization of transition metal complexes may be useful in the design of new systems with long-lived excited states for photodynamic therapy.

Introduction

Complexes with extended π systems are known to exhibit strong binding to DNA through intercalation and, in some cases, display enhanced emission when bound to DNA.[1−9] Weakly or nonemissive complexes that become highly luminescent in the presence of double-stranded DNA may have potential applications related to various biomedical fields,[10−13] including electrochemical sensors for specific DNA sequences, hybridization,[14] and base pair mismatches.[15,16] Another important aspect of molecules with long-lived excited states is their potential for generation of $^1O_2$, the reactive species produced upon irradiation by current agents used for photodynamic therapy (PDT).[17]

It was found recently that a Ru(II) complex derived from the tridentate tpy ligand, $[Ru(tpy)(pydppz)]^{2+}$ (tpy =

* Authors to whom correspondence should be addressed. E-mail: turro@chemistry.ohio-state.edu (C.T.), thummel@uh.edu (R.P.T.).
† The Ohio State University.
‡ University of Houston.

(1) (a) Friedman, A. E.; Chambron, J. C.; Sauvage, J. P.; Turro, N. J.; Barton, J. K. *J. Am. Chem. Soc.* **1990**, *112*, 4960. (b) Jenkins, Y.; Barton, J. K. *J. Am. Chem. Soc.* **1992**, *114*, 8736. (c) Hartshorn, R. M.; Barton, J. K. *J. Am. Chem. Soc.* **1992**, *114*, 5919–25. (d) Jenkins, Y.; Friedman, A. E.; Turro, N. J.; Barton, J. K. *Biochemistry* **1992**, *31*, 10809. (e) Holmlin, R. E.; Barton, J. K. *Inorg. Chem.* **1995**, *34*, 7. (f) Olson, E. J. C.; Hu, D.; Hoermann, A.; Jonkman, A. M.; Arkin, M. R.; Stemp, E. D. A.; Barton, J. K.; Barbara, P. F. *J. Am. Chem. Soc.* **1997**, *119*, 11458. (g) Holmlin, R. E.; Stemp, E. D. A.; Barton, J. K. *Inorg. Chem.* **1998**, *37*, 29.
(2) Brennaman, M. K.; Alstrum-Acevedo, J. H.; Fleming, C. N.; Jang, P.; Meyer, T. J.; Papanikolas, J. M. *J. Am. Chem. Soc.* **2002**, *124*, 15094.
(3) Moucheron, C.; Kirsch-De Mesmaeker, A.; Choua, S. *Inorg. Chem.* **1997**, *36*, 584.
(4) (a) Olofsson, J.; Oenfelt, B.; Lincoln, P. *J. Phys. Chem. A* **2004**, *108*, 4391. (b) Olofsson, J.; Wilhelmsson, L. M.; Lincoln, P. *J. Am. Chem. Soc.* **2004**, *126*, 15458. (c) Westerlund, F.; Pierard, F.; Eng, M. P.; Norden, B.; Lincoln, P. *J. Phys. Chem. B* **2005**, *109*, 17327. (d) Westerlund, F.; Eng, M. P.; Winters, M. U.; Lincoln, P. *J. Phys. Chem. B* **2007**, *111*, 310.
(5) Nair, R. B.; Murphy, C. J. *J. Inorg. Biochem.* **1998**, *69*, 129.
(6) (a) Coates, C. G.; McGarvey, J. J.; Callaghan, P. L.; Coletti, M.; Hamilton, J. G. *J. Phys. Chem. B* **2001**, *105*, 730. (b) Coates, C. G.; Callaghan, P.; McGarvey, J. J.; Kelly, J. M.; Jacquet, L.; Kirsch-De Mesmaeker, A. *J. Mol. Struct.* **2001**, *598*, 15. (c) Coates, C. G.; Olofsson, J.; Coletti, M.; McGarvey, J. J.; Oenfelt, B.; Lincoln, P.; Norden, B.; Tuite, E.; Matousek, P.; Parker, A. W. *J. Phys. Chem. B* **2001**, *105*, 12653.
(7) Li, J.; Chen, J.-C.; Xu, L.-C.; Zheng, K.-C.; Ji, L.-N. *J. Organomet. Chem.* **2007**, *692*, 831.
(8) Foxon, S. P.; Phillips, T.; G., Martin, R.; Towrie, M.; Parker, A. W.; Webb, M.; Thomas, J. A. *Angew. Chem., Int. Ed.* **2007**, *46*, 3686.

10.1021/ic801636u CCC: $40.75
Published on Web 11/26/2008

Scheme 1

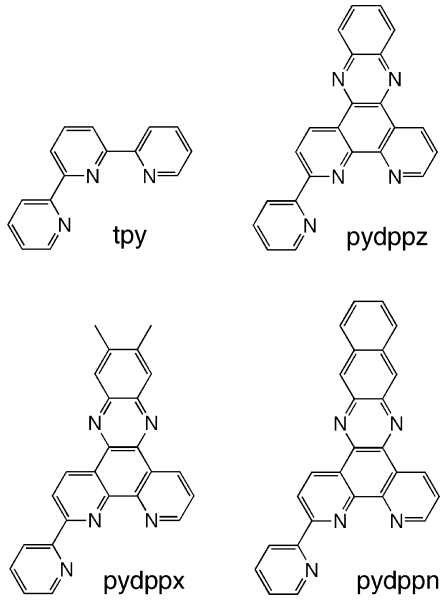

[2,2′;6′,2″]-terpyridine, pydppz = 3-(pyrid-2′-yl)dipyrido[3,2-*a*:2′,3′-*c*]phenazine) also shows "light-switch" behavior.[18] The structure of the pydppz ligand is shown in Scheme 1. The lowest energy emissive excited states in $[Ru(tpy)(pydppz)]^{2+}$ and the homoleptic complexes $[Ru(tpy)_2]^{2+}$ and $[Ru(pydppz)_2]^{2+}$ are known to be metal-to-ligand charge transfer (^{3}MLCT) in nature, which is typical for these and related Ru(II) complexes.[18] The ^{3}MLCT lifetimes of $[Ru(tpy)(pydppz)]^{2+}$ and $[Ru(pydppz)_2]^{2+}$ were previously measured to be ~5 and 2.4 ns, respectively.[18] The excited state lifetimes of these systems are too short for efficient bimolecular energy transfer to generate $^1O_2$, making them less useful as potential PDT agents.

The present paper explores the excited state properties of related Ru(II) complexes possessing pydppx (3-(pyrid-2′-yl)-11,12-dimethyl-dipyrido[3,2-*a*:2′,3′-*c*]phenazine) and pydppn (3-(pyrid-2′-yl)-4,5,9,16-tetraaza-dibenzo[*a*,*c*]naphthacene) ligands (Scheme 1). Ru(II) complexes possessing the pydppx ligand are similar to the pydppz systems, with lowest energy ^{3}MLCT excited state with lifetimes of 1−4 ns. Unlike their pydppz and pydppx counterparts, the lowest energy excited state in the $[Ru(tpy)_n(pydppn)_{2-n}]^{2+}$ ($n = 0$, 1) complexes is a ligand-centered (LC) $^3\pi\pi^*$ localized on the pydppn ligand with microsecond lifetimes. These complexes are able to generate $^1O_2$ in high yield, which may make them useful in the design of new metal complexes with long-lived excited states for PDT.

Experimental Section

Materials. Sodium chloride, sodium phosphate, gel loading buffer (0.05% (w/v) bromophenol blue, 40% (w/v) sucrose, 0.1 M ethylenediaminetetraacetic acid (EDTA), 0.5% (w/v) sodium lauryl sulfate), tris-hydroxymethyl-aminomethane (Tris base), Tris/HCl, and ethidium bromide were purchased from Sigma-Aldrich and used as received. Calf-thymus DNA was purchased from Sigma and was dialyzed against a 5 mM Tris, 50 mM NaCl (pH = 7.5) buffer three times during a 48 h period prior to use. The concentration of the resulting DNA solution was calculated from its absorption at 260 nm (A_{260}) with $\varepsilon = 6600\ M^{-1}\ cm^{-1}$, and its purity was verified by the relative absorption at 260 and 280 nm ($A_{260}/A_{280} \geq 1.8$). The pUC18 plasmid was purchased from Bayou Biolabs and purified using the Concert Miniprep System from Life Technologies. Acetonitrile was dried over CaH_2 and distilled under an argon atmosphere prior to use. $RuCl_3 \cdot 3H_2O$, KBr, 2,3-diaminonaphthalene, 4,5-dimethyl-1,2-phenylenediamine, *o*-phenylenediamine, [2,2′;6′,2″]-terpyridine (tpy), and NH_4PF_6 were commercially available. $Ru(tpy)Cl_3$,[19] 2-(pyrid-2′-yl)-1,10-phenanthroline,[20] and 2-(pyrid-2′-yl)-1,10-phenanthroline-5,6-dione[18] were synthesized by methods previously reported. The microwave reactions were carried out in a household microwave oven modified according to a published description.[21]

3-(Pyrid-2′-yl)-4,5,9,16-tetraaza-dibenzo[*a*,*c*]naphthacene (pydppn). A mixture of 2,3-diaminonaphthalene (142 mg, 0.90 mmol) and 2-(pyrid-2′-yl)-1,10-phenanthroline-5,6-dione (100 mg, 0.34 mmol) suspended in 15 mL of ethanol was heated to reflux and stirred under Ar for 2 h. The reaction mixture was filtered, and the solid was washed with ethanol and acetone, then dried under a vacuum to provide pydppn as orange flakes (0.120 g, 84%), mp >305 °C. ^{1}H NMR ($CDCl_3$): δ 9.75 (d, 1 H, J = 8.4 Hz), 9.69 (dd, 1 H, J = 1.5, 8.4 Hz), 9.30 (d, 1 H, J = 5.1 Hz), 9.01 (d, 1 H, J = 7.5 Hz), 8.97 (s, 1 H), 8.95 (s, 1 H), 8.94 (d, 1 H, J = 8.1 Hz), 8.79 (ddd, 1 H, J = 0.9, 1.8, 5.4 Hz), 8.20 (m, 2 H), 7.97 (dt, 1 H, J = 1.5, 7.8 Hz), 7.83 (dd, 1 H, J = 4.5, 7.8 Hz), 7.63 (dd, 2 H, J = 3.0, 6.6 Hz), 7.43 (ddd, 1 H, J = 0.9, 4.5, 9.0 Hz). ^{13}C NMR could not be obtained due to poor solubility. IR: 1590, 1387, 1359, 1089, 874, 749 cm^{-1}. Anal. calcd for $C_{27}H_{15}N_5 \cdot 1.25H_2O$: C, 75.07; H, 4.08; N, 16.21. Found: C, 74.96; H, 3.66; N, 16.03.

3-(Pyrid-2′-yl)-11,12-dimethyl-dipyrido[3,2-*a*:2′,3′-*c*]phenazine (pydppx). In a manner similar to that described for pydppn, 4,5-dimethyl-1,2-phenylenediamine (122 mg, 0.90 mmol) and 2-(pyrid-2′-yl)-1,10-phenanthroline-5,6-dione (100 mg, 0.34 mmol) were refluxed in 15 mL of ethanol for 2 h to provide pydppx as yellow flakes (0.118 g, 87%), mp >305 °C. ^{1}H NMR ($CDCl_3$): δ 9.73 (d, 1 H, J = 8.4 Hz), 9.67 (dd, 1 H, J = 1.8, 8.1 Hz), 9.31 (dd, 1 H, J = 1.8, 4.5 Hz), 9.01 (d, 1 H, J = 8.4 Hz), 8.93 (d, 1 H, J = 8.1 Hz), 8.79 (d, 1 H, J = 4.8 Hz), 8.11 (s, 1 H), 8.09 (s, 1 H), 7.96 (td, 1 H, J = 1.5, 8.1 Hz), 7.81 (dd, 1 H, J = 4.5, 8.1 Hz), 7.42 (ddd, 1 H, J = 1.5, 4.8, 7.8 Hz), 2.61 (s, 6H). ^{13}C NMR could not be obtained due to poor solubility. IR: 1590, 1481, 1387, 1360, 1091, 860, 751 cm^{-1}. Anal. calcd for $C_{25}H_{17}N_5$: C, 77.52, H, 4.39, N, 18.09. Found: C, 77.61, H, 3.92, N, 17.69.

(9) Atsumi, M.; Gonzalez, L.; Daniel, C. *J. Photochem. Photobiol., A: Chemistry* **2007**, *190*, 310.
(10) Chen, F.; Ai, X.-P.; He, Z.-K.; Li, M.-J.; Chen, X.-D. *Spectrosc. Lett.* **2005**, *38*, 99.
(11) Jiang, Y.; Fang, X.; Bai, C. *Anal. Chem.* **2004**, *76*, 5230.
(12) Arounaguiri, S.; Maiya, B. G. *Inorg. Chem.* **1999**, *38*, 842.
(13) Zou, X.-H.; Ji, L.-N. *Trends Inorg. Chem.* **2001**, *7*, 99.
(14) Marti, A. A.; Puckett, C. A.; Dyer, J.; Stevens, N.; Jockusch, S.; Ju, J.; Barton, J. K.; Turro, N. J. *J. Am. Chem. Soc.* **2007**, *129*, 8680.
(15) Rueba, E.; Hart, J. R.; Barton, J. K. *Inorg. Chem.* **2004**, *43*, 4570–4578.
(16) Ling, L.-S.; He, Z.-K.; Chen, F.; Zeng, Y.-E. *Talanta* **2003**, *59*, 269–275.
(17) Detty, M. R.; Gibson, S. L.; Wagner, S. J. *J. Med. Chem.* **2004**, *47*, 3897–3915.
(18) Liu, Y.; Hammitt, R.; Lutterman, D. A.; Thummel, R. P.; Turro, C. *Inorg. Chem.* **2007**, *46*, 6011–6021.
(19) Sullivan, B. P.; Calvert, J. M.; Meyer, T. J. *Inorg. Chem.* **1980**, *19*, 1404–1407.
(20) Hung, C.-Y.; Wang, T.-L.; Shi, Z.; Thummel, R. P. *Tetrahedron* **1994**, *50*, 10685–92.
(21) Matsumura-Inoue, T.; Tanabe, M.; Minami, T.; Ohashi, T. *Chem. Lett.* **1994**, 2443–6.

[Ru(pydppn)$_2$](PF$_6$)$_2$. $RuCl_3 \cdot 3H_2O$ (10.7 mg, 0.051 mmol) and ethylene glycol (2.5 mL) were added to pydppn (42 mg, 0.10 mmol). The suspension was heated in a microwave oven for 30 min and then added to NH_4PF_6 (34 mg, 0.20 mmol) in water (10 mL). The suspension was filtered and washed with ethanol and ether. The solid was then dissolved in CH_3CN and purified by chromatography on alumina (15 g). Eluting with CH_3CN provided [Ru(pydppn)$_2$](PF$_6$)$_2$ as a red solid (24 mg, 39%). ^{1}H NMR (CD_3CN): δ 9.87 (d, 1 H, J = 8.7 Hz), 9.45 (dd, 1 H, J = 1.2, 8.4 Hz), 9.25 (s, 1 H), 9.21 (d, 1 H, J = 8.7 Hz), 9.14 (s, 1 H), 8.74 (d, 1 H, J = 7.8 Hz), 8.42 (m, 2 H), 8.01 (td, 1 H, J = 1.5, 7.8 Hz), 7.82 (m, 3 H), 7.56 (d, 1 H, J = 5.1 Hz), 7.55 (dd, 1 H, J = 5.4, 8.1 Hz), 7.18 (ddd, 1 H, J = 0.9, 5.7, 7.5 Hz). ESI MS: m/z 1065, [Ru(pydppn)$_2$](PF$_6$)$^+$; 462, [Ru(pydppn)$_2$]$^{2+}$.

[Ru(pydppx)$_2$](PF$_6$)$_2$. A procedure similar to that described for [Ru(pydppn)$_2$](PF$_6$)$_2$ was followed, using $RuCl_3 \cdot 3H_2O$ (13.7 mg, 0.066 mmol), ethylene glycol (2.5 mL), and pydppx (51 mg, 0.13 mmol), to provide [Ru(pydppx)$_2$](PF$_6$)$_2$ as a red solid (61 mg, 79%). ^{1}H NMR (CD_3CN): δ 9.84 (d, 1 H, J = 8.7 Hz), 9.40 (dd, 1 H, J = 0.9, 8.4 Hz), 9.19 (d, 1 H, J = 9.0 Hz), 8.72 (d, 1 H, J = 7.2 Hz), 8.33 (s, 1 H), 8.21 (s, 1 H), 7.98 (td, 1 H, J = 1.2, 8.1 Hz), 7.74 (dd, 1 H, J = 1.5, 5.7 Hz), 7.49 (d, 1 H, J = 5.4 Hz), 7.49 (dd, 1 H, J = 5.1, 8.1 Hz), 7.12 (ddd, 1 H, J = 1.2, 5.7, 7.8 Hz), 2.71 (s, 3 H), 2.68 (s, 3 H). ESI MS: m/z 1021, [Ru(pydppx)$_2$](PF$_6$)$^+$, 462, [Ru(pydppx)$_2$]$^{2+}$. Anal. calcd for $C_{50}H_{34}N_{10}RuP_2F_{12} \cdot H_2O$: C, 50.72; H, 3.04; N, 11.83. Found: C, 50.82; H, 2.58; N, 11.77.

[Ru(tpy)(pydppn)](PF$_6$)$_2$. A suspension of pydppn (77 mg, 0.19 mmol) and [Ru(tpy)Cl$_3$] (54 mg, 0.13 mmol) in ethanol/water (1:1 v/v, 20 mL) was stirred at reflux under Ar for 21 h. The ethanol was evaporated, and the solution was added dropwise to NH_4PF_6 (200 mg, 1.20 mmol) in water (5 mL). The precipitate was filtered, washed with ether, and purified by chromatography on silica gel, eluting with CH_3CN/1 M $NaNO_3$ (4:1). Precipitation using NH_4PF_6 provided [Ru(tpy)(pydppn)](PF$_6$)$_2$ as a red solid (72 mg, 56%), mp >270 °C. ^{1}H NMR (CD_3CN): δ 9.79 (d, 1 H, J = 8.4 Hz), 9.45 (dd, 1 H, J = 1.2, 7.8 Hz), 9.23 (s, 1 H), 9.13 (d, 1 H, J = 8.4 Hz), 9.13 (s, 1 H), 8.80 (d, 2 H, J = 8.4 Hz), 8.68 (d, 1 H, J = 7.8 Hz), 8.47 (m, 5 H), 8.00 (td, 1 H, J = 1.2, 7.8 Hz), 7.89 (td, 2 H, J = 1.2, 8.1 Hz), 7.77 (m, 3 H), 7.60 (dd, 1 H, J = 5.1, 7.8 Hz), 7.50 (dd, 1 H, J = 0.9, 5.4 Hz), 7.36 (d, 2 H, J = 6.0 Hz), 7.23 (ddd, 1 H, J = 2.1, 5.7, 7.8 Hz), 7.06 (ddd, 2 H, J = 2.1, 5.1, 7.5 Hz).

[Ru(tpy)(pydppx)](PF$_6$)$_2$. A procedure similar to that described for [Ru(tpy)(pydppn)](PF$_6$)$_2$ was followed, using ethanol/water (1:1 v/v, 20 mL), pydppx (88 mg, 0.23 mmol), and [Ru(tpy)Cl$_3$] (66 mg, 0.15 mmol) to afford a red solid, [Ru(tpy)(pydppx)](PF$_6$)$_2$ (64 mg, 42%), mp >270 °C. ^{1}H NMR (CD_3CN): δ 9.76 (d, 1 H, J = 8.7 Hz), 9.41 (dd, 1 H, J = 1.2, 8.1 Hz), 9.12 (d, 1 H, J = 8.7 Hz), 8.80 (d, 2 H, J = 8.1 Hz), 8.67 (d, 1 H, J = 7.5 Hz), 8.51 (d, 2 H, J = 8.1 Hz), 8.45 (t, 1 H, J = 7.8 Hz), 8.30 (s, 1 H), 8.21 (s, 1 H), 7.99 (td, 1 H, J = 1.2, 8.1 Hz), 7.89 (td, 2 H, J = 1.2, 8.1 Hz), 7.75 (dd, 1 H, J = 1.2, 5.7 Hz), 7.59 (dd, 1 H, J = 5.4, 8.1 Hz), 7.49 (d, 1 H, J = 5.4 Hz), 7.32 (d, 2 H, J = 5.7 Hz), 7.22 (ddd, 1 H, J = 1.2, 5.4, 7.5 Hz), 7.04 (ddd, 2 H, J = 1.2, 5.7, 8.1 Hz). Anal. calcd for $C_{40}H_{28}N_8RuP_2F_{12} \cdot 1.5H_2O$: C, 46.24; H, 2.99; N, 10.79. Found: C, 46.15; H, 2.58; N, 10.53.

Instrumentation. ^{1}H NMR spectra were recorded on a General Electric QE-300 spectrometer at 300 MHz, and chemical shifts were referenced to the residual solvent peak. IR spectra were recorded on a Thermo-Finnigan 370 FT-IR. Melting points were measured with a Thomas-Hoover capillary melting point apparatus and are uncorrected. Mass spectra were obtained on a Thermo Finnigan LCQ Deca XP Plus with a Surveyor LC-MS. Elemental analysis was performed by QTI, Whitehouse, New Jersey.

Electrochemical studies were carried out on a BAS Epsilon or CV-50W voltammetric analyzer in a three-electrode cell with a glassy carbon working electrode, a Pt wire auxiliary electrode, and a saturated calomel electrode (SCE) as the reference electrode; the latter was separated from the bulk solution by a glass frit. The measurements were conducted at a scan rate of 100 mV/s in deoxygenated, anhydrous CH_3CN containing 0.1 M tetra-*n*-butylammonium hexafluorophosphate as the supporting electrolyte. The oxidation potential of ferrocene (0.42 V vs SCE)[22] was measured separately under identical conditions and was used as an internal reference.

Steady-state absorption spectra were recorded on a Perkin-Elmer Lambda 900 spectrometer or a HP diode array spectrometer (HP 8453) with HP8453 Win System software. Corrected steady-state emission spectra were measured on a SPEX Fluoromax-2 or a Perkin-Elmer LS50B Luminescence spectrometer. Femtosecond transient absorption spectra were recorded on a home-built instrument with a CCD detector previously described in detail (fwhm $\approx$ 300 fs).[23] The home-built transient absorption instrument for measurements on the nanosecond and microsecond timescales was previously reported, and excitation was accomplished through the use of a frequency-doubled (532 nm) or -tripled (355 nm) Spectra-Physics GCR-150 Nd:YAG laser (fwhm $\sim$ 8 ns).[24]

A 150 W Xe arc lamp in a PTI housing (Milliarc Compact Lamp Housing) powered by an LPS-220 power supply (PTI) with an LPS-221 igniter (PTI) was used for the DNA photocleavage. The irradiation wavelength was selected by placing long-pass colored glass filters (Melles Griot) and a 10 cm water cell in the light path. The ethidium bromide stained agarose gels were imaged using a GelDoc 2000 transilluminator (BioRad) equipped with Quality One (v. 4.0.3) software.

Methods. Photophysical measurements were performed in a 1 $\times$ 1 cm quartz cuvette equipped with a rubber septum, and the solutions were bubbled with Ar for 15 min prior to each measurement, unless otherwise noted. For the emission measurements, sample concentrations were adjusted to produce solutions with absorption at the excitation wavelength < 0.20, which resulted in concentrations of $\sim$15 μM. Emission quantum yields were measured using [Ru(bpy)$_3$]$^{2+}$ in oxygen-free CH_3CN (Φ = 0.062) as the actinometer.[25] The transient absorption measurements were performed on solutions with an absorption of 0.3−0.8 at the excitation wavelength. A Harrick Scientific flow cell equipped with 1 mm CaF_2 windows (1 mm path length) was used for the ultrafast transient absorption experiments. The polarization angle between the pump and probe beams was 54.7° to avoid rotational diffusion effects. The samples were excited at 310 nm, with pump pulse energy at the sample position of $\sim$6 μJ (fwhm $\approx$ 300 fs), and the spectra were corrected for the chirp in the probe continuum.[26] Kinetic traces were analyzed by fitting to a sum of exponential terms, $S(t) = \sum A_i \exp(-t/\tau_i) + C$ (independent amplitudes, A_i, lifetimes, τ_i, and an offset, C). Convolution with a Gaussian response function was included in the fit.

(22) Gagne, R. R.; Koval, C. A.; Lisensky, G. C. *Inorg. Chem.* **1980**, *19*, 2854.
(23) Burdzinski, G.; Hackett, J. C.; Wang, J.; Gustafson, T. L.; Hadad, C. M.; Platz, M. S. *J. Am. Chem. Soc.* **2006**, *128*, 13402–13411.
(24) Warren, J. T.; Chen, W.; Johnston, D. H.; Turro, C. *Inorg. Chem.* **1999**, *38*, 6187–6192.
(25) Caspar, J. V.; Meyer, T. J. *J. Am. Chem. Soc.* **1983**, *105*, 5583–90.
(26) Nakayama, T.; Amijima, Y.; Ibuki, K.; Hamanoue, K. *Rev. Sci. Instrum.* **1997**, *68*, 4364–4371.

Scheme 2

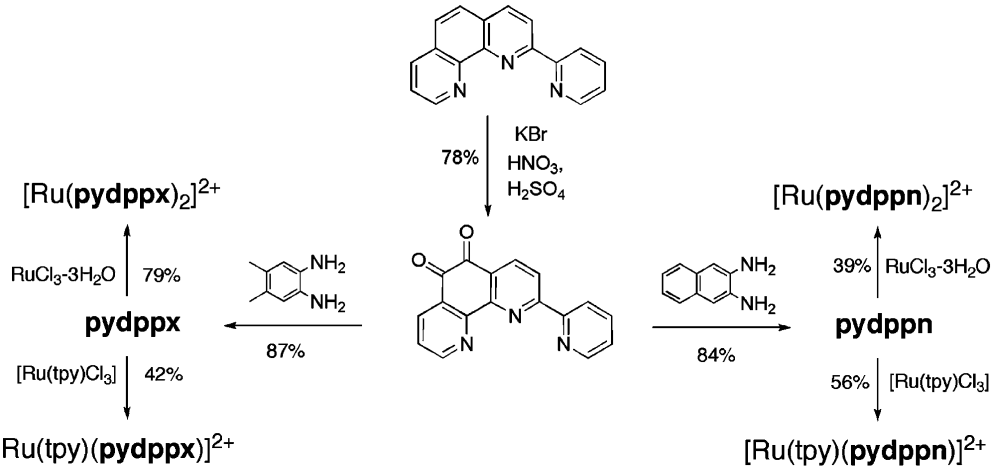

The binding constants of the metal complexes to DNA determined by absorption and emission titrations at room temperature were measured with a ~10 μM metal complex, and the concentration of calf-thymus DNA was varied from 0 to 100 μM (5 mM Tris/HCl, 50 mM NaCl, pH 7.5). The dilution of the metal complex at the end of each titration was negligible. The DNA binding constants, K_b, were obtained from fits of the titration data, as previously reported.[18,27−29] DNA photocleavage experiments were carried out using a 20 μL total sample volume in 0.5 mL transparent Eppendorf tubes containing 100 μM pUC18 plasmid and various concentrations of each metal complex (5 mM Tris, pH = 7.5, 50 mM NaCl). Irradiation of the solutions was performed either in air, under a positive pressure of argon following bubbling for ~15 min, or after five freeze−pump−thaw cycles in a quartz tube equipped with a Kontes stopcock (using ~3-fold greater solution volume). After irradiation, 4 μL of the DNA gel loading buffer was added to each 20 μL sample. The electrophoresis was carried out using a 1% agarose gel stained with 0.5 mg/L ethidium bromide in TAE buffer (40 mM Tris-acetate, 1 mM EDTA, pH = 8.2).

Results and Discussion

Synthesis. The synthetic strategy for the preparation of the ligands and complexes was similar to that reported previously for pydppz.[18] The key starting compound, 2-(pyrid-2′-yl)-1,10-phenanthroline, was synthesized from the Friedländer condensation of 8-amino-7-quinolinecarbaldehyde with 2-acetylpyridine.[20,30] Oxidation of 2-(pyrid-2′-yl)-1,10-phenanthroline with KBr in a mixture of nitric and sulfuric acid results in the formation of 2-(pyrid-2′-yl)-1,10-phenanthroline-5,6-dione in 78% yield. This dione was then condensed with 4,5-dimethyl-1,2-phenylenediamine and 2,3-diaminonaphthalene to produce the target ligands, pydppx and pydppn, in yields of 87% and 84%, respectively (Scheme 2). Pydppx and pydppn were characterized by ^{1}H NMR, IR, and elemental analysis. Treatment of pydppx or pydppn with $RuCl_3 \cdot 3H_2O$ in ethylene glycol under microwave irradiation produces the homoleptic complexes, $[Ru(pydppx)_2]^{2+}$ and $[Ru(pydppn)_2]^{2+}$ in yields of 79% and 39%, respectively. The treatment of pydppx or pydppn with $[Ru(tpy)Cl_3]$ in refluxing aqueous ethanol provided the heteroleptic complexes $[Ru(tpy)(pydppx)]^{2+}$ and $[Ru(tpy)(pydppn)]^{2+}$ in yields of 42% and 56%, respectively. The complexes were initially precipitated as their PF_6 salts by treatment with ammonium hexafluorophosphate and later metathesized back to their chloride salts to provide the samples used for DNA photocleavage studies.

The complexes were identified primarily by their ^{1}H NMR spectra in CD_3CN solution. The homoleptic $[Ru(pydppn)_2]^{2+}$ and $[Ru(pydppx)_2]^{2+}$ complexes each possess a C_2 symmetry axis, and therefore the two ligands in each complex are magnetically equivalent and exhibit a single set of resonances. For $[Ru(pydppx)_2]^{2+}$, one finds two, three, and four proton patterns that are typical of interacting pyridine ring protons. The protons on the terminal dimethylbenzo ring appear as singlets at 8.33 and 8.21 ppm, while the methyl groups exhibit three proton singlets at 2.71 and 2.68 ppm. The spectrum of $[Ru(pydppn)_2]^{2+}$ is somewhat more complex because of the four additional signals from the fused naphtho ring. For the heteroleptic complexes $[Ru(pydppx)(tpy)]^{2+}$ and $[Ru(pydppn)(tpy)]^{2+}$, the pydppx or pydppn ligand exhibits a pattern very similar to what is found for the homoleptic complexes superimposed on six resonances for the auxiliary tpy. The integration of five of these tpy signals corresponds to two protons each, making them readily distinguishable from the one-proton pydppx and pydppn peaks.

Electrochemistry, Electronic Absorption, and Emission. The oxidation and reduction potentials of $[Ru(L)_2]^{2+}$ (L = tpy, pydppx, pydppn) and $[Ru(tpy)(L)]^{2+}$ (L = pydppx, pydppn) complexes in CH_3CN are listed in Table 1. The complexes display a single and reversible oxidation wave in the range of +1.31 to +1.41 V versus SCE (Table 1), which can be assigned to the Ru(III/II) couple. The value measured for $[Ru(tpy)_2]^{2+}$, $E_{1/2}([Ru]^{3+/2+})$ = +1.38 V versus SCE in CH_3CN, is consistent with that previously reported for this complex.[31,32] The oxidation potentials listed in Table 1 are similar to those measured for the related $[Ru(tpy)_n(pydppz)_{2-n}]^{2+}$ (n = 0, 1) series.[18] It is

(27) Carter, M. T.; Rodriguez, M.; Bard, A. J. *J. Am. Chem. Soc.* **1989**, *111*, 8901–11.
(28) Kalsbeck, W. A.; Thorp, H. H. *J. Am. Chem. Soc.* **1993**, *115*, 7146–51.
(29) Chouai, A.; Wicke, S. E.; Turro, C.; Bacsa, J.; Dunbar, K. R.; Wang, D.; Thummel, R. P. *Inorg. Chem.* **2005**, *44*, 5996–6003.
(30) Riesgo, E. C.; Jin, X.; Thummel, R. P. *J. Org. Chem.* **1996**, *61*, 3017–22.

Table 1. Photophysical Data and Electrochemistry of $[Ru(tpy)_n(L)_{2-n}]^{2+}$ (L = pydppx, pyppn; n = 0−2)

complex	λ_{abs}/nm ($\varepsilon \times 10^3$ M^{-1} cm^{-1})[a]	λ_{em}/nm (Φ_{em})[a,b]	λ_{em}/nm ($\tau/\mu s$)[c]	τ_{TA}[d]	$E_{1/2}$/V[e]
$[Ru(tpy)_2]^{2+}$	269 (25.8), 308 (38.4), 476 (14.4)	629[d] (<5 × 10^{-6})[f]	598(10.8)	120 ps	+1.38,−1.21
$[Ru(tpy)(pydppx)]^{2+}$	305 (77.3), 368 (22.4), 385 (22.9), 473 (17.6)	713 (3.5 × 10^{-4})	644(6.85)	3.7 ns	+1.31,−0.99
$[Ru(pydppx)_2]^{2+}$	302 (85.5), 385 (36.0), 479 (18.2)	690 (1.3 × 10^{-4})	640(6.54)	1.1 ns	+1.38,−0.96
$[Ru(tpy)(pydppn)]^{2+}$	331 (60.1), 390 (12.6), 414 (11.5), 474 (16.8)	703 (3.0 × 10^{-5})	648(6.64)	20.1μs	+1.35,−0.70
$[Ru(pydppn)_2]^{2+}$	289 (42.4), 344 (64.9), 415 (12.1), 477 (14.5)	[g]	[g]	24.3μs	+1.41,−0.66

[a] H_2O. [b] 298 K. [c] Ethanol/methanol (v/v 4:1), 77 K. [d] CH_3CN. [e] CH_3CN, 0.1 M Bu_4NPF_6, vs SCE. [f] From ref . [g] Not observed.

interesting to note that the heteroleptic complexes are slightly easier to oxidize than their homoleptic counterparts. The $[Ru(L)_2]^{2+}$ (L = tpy, pydppx, pydppn) and $[Ru(tpy)(L)]^{2+}$ (L = pydppx, pydppn) complexes exhibit well-resolved reversible ligand-centered reduction waves. $[Ru(tpy)_2]^{2+}$ displays a reduction with $E_{1/2}([Ru]^{2+/+}) = -1.21$ V versus SCE, consistent with the reported value.[33] The cathodic waves in the homoleptic complexes are observed at −0.96 V versus SCE for $[Ru(pydppx)_2]^{2+}$ and −0.66 V versus SCE for $[Ru(pydppn)_2]^{2+}$, while they were measured at −0.99 V versus SCE and at −0.70 V versus SCE in the heteroleptic systems $[Ru(tpy)(pydppx)]^{2+}$ and $[Ru(tpy)(pydppn)]^{2+}$, respectively. These results are consistent with the localization of the electron on the pydppn ligand in $[Ru(tpy)_n(pydppn)_{2-n}]^{2+}$ (n = 0,1) and on the pydppx ligand in the $[Ru(tpy)_n(pydppx)_{2-n}]^{2+}$ (n = 0, 1) complexes (Table 1).

The pydppn ligand coordinated to Ru(II) is easier to reduce than pydppz and pydppx, following the trend pydppn > pydppz > pydppx, which is consistent with previously reported data for the related complexes. For example, in $[Ru(bpy)_2L]^{2+}$, where L = dpq (dipyrido[3,2-*d*:2′,3′-*f*]quinoxaline), dppz (dipyrido[3,2-*a*:2′,3′-*c*]phenazine), and dppx (11,12-dimethyl-dipyrido[3,2-*a*:2′,3′-*c*]phenazine), with respective reduction potentials at −1.04, −0.73, and −0.81 V versus NHE,[34] show that the smaller dpq ligand is more difficult to reduce than dppz. Similarly, the large aromatic pydppn ligand provides a greater area for charge delocalization compared to pydppz, making the former easier to reduce than the latter. The electron-donating substitutents on the pydppx ligand increase the electron density on the ring, resulting in a more negative $E_{1/2}([Ru]^{2+/+})$ value compared to pydppz. These results are similar to those for $[Ru(bpy)_2L]^{2+}$ (L = dppz, dppx) discussed above.[34]

The absorption maxima (λ_{abs}) and molar extinction coefficients (ε) of $[Ru(tpy)_n(L)_{2-n}]^{2+}$ (L = pydppx, pydppn; n = 0−2) complexes are listed in Table 1, and the absorption spectra of the representative complexes $[Ru(tpy)(pydppn)]^{2+}$ and $[Ru(tpy)(pydppx)]^{2+}$ are shown in Figure 1 in CH_3CN. The peaks observed at 368 and 385 nm in $[Ru(tpy)_n(pydppx)_{2-n}]^{2+}$ (n = 0, 1) can be ascribed to $^1\pi\pi^*$ transitions of the pydppx ligand, since absorption maxima of the free pydppx ligand are observed at 288 (ε = 39 000 M^{-1} cm^{-1}), 375 (ε = 16 000 M^{-1} cm^{-1}), and 395 nm (ε = 20 000 M^{-1} cm^{-1}). For $[Ru(tpy)_n(pydppn)_{2-n}]^{2+}$ (n = 0, 1), the $^1\pi\pi^*$ transitions of the pydppn ligand are observed at 331−344, 390, and ∼415 nm, which are at similar energies to absorption maxima of the pydppn ligand in $CHCl_3$, observed at 329 (ε = 66 000 M^{-1} cm^{-1}), 398 (ε = 13 000 M^{-1} cm^{-1}), and 421 nm (ε = 17 000 M^{-1} cm^{-1}). It should be noted that lowest LC $^1\pi\pi^*$ transitions shift to higher energy upon coordination to the Ru(II) center, from 395 to 385 nm for pydppx and from 421 to 415 nm for pydppn. A similar shift of the dppz-centered lowest-energy transition was reported for $[Ru(phen)_2(dppz)]^{2+}$.[35] The ^{1}MLCT absorption is observed at ∼475 nm in the $[Ru(tpy)_n(L)_{2-n}]^{2+}$ (L = pydppx, pyddpn; n = 0,1), consistent with that in $[Ru(tpy)_2]^{2+}$ at 476 nm.[32]

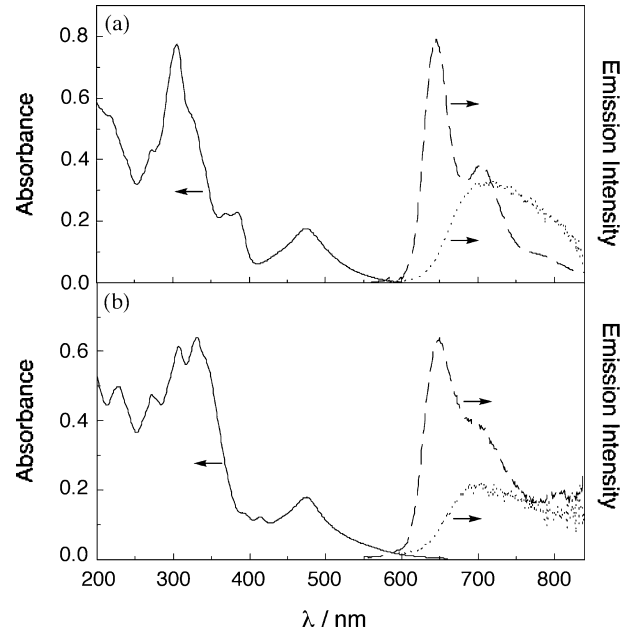

Figure 1. Electronic absorption (—) and emission (•••) spectra at 298 K in water (λ_{exc} = 475 nm, 12 μM) and at 77 K (---, λ_{exc} = 475 nm, 35 μM) in ethanol/methanol (v/v 4:1) glasses of (a) $[Ru(tpy)(pydppx)]^{2+}$ and (b) $[Ru(tpy)(pydppn)]^{2+}$.

The emission spectra of 12 μM $[Ru(tpy)(pydppx)]^{2+}$ and $[Ru(tpy)(pydppn)]^{2+}$ at 298 K in water and at 77 K in an ethanol/methanol (v/v = 4:1) glasses are also illustrated in Figure 1. Luminescence was not detected for 11 μM $[Ru(pydppn)_2]^{2+}$ at 298 K in water or at 77 K in an ethanol/methanol (v/v = 4:1) glass (λ_{exc} = 475). Weak luminescence was detected for $[Ru(tpy)(pydppx)]^{2+}$, $[Ru(pydppx)_2]^{2+}$, and $[Ru(tpy)(pydppn)]^{2+}$ at room temperature with maxima and quantum yields listed in Table 1, along with measurements

(31) Maestri, M.; Armaroli, N.; Balzani, V.; Constable, E. C.; Thompson, A. M. W. C. *Inorg. Chem.* **1995**, *34*, 2759–67.
(32) (a) Lin, C. T.; Boettcher, W.; Chou, M.; Creutz, C.; Sutin, N. *J. Am. Chem. Soc.* **1976**, *98*, 6536–44. (b) Creutz, C.; Chou, M.; Netzel, T. L.; Okumura, M.; Sutin, N. *J. Am. Chem. Soc.* **1980**, *102*, 1309–19.
(33) Benniston, A. C.; Grosshenny, V.; Harriman, A.; Ziessel, R. *Dalton Trans.* **2004**, 1227–1232.
(34) Delaney, S.; Pascaly, M.; Bhattacharya, P. K.; Han, K.; Barton, J. K. *Inorg. Chem.* **2002**, *41*, 1966–1974.
(35) Hiort, C.; Lincoln, P.; Norden, B. *J. Am. Chem. Soc.* **1993**, *115*, 3448–54.

at 77 K. The values for the pydppx complexes are comparable to those of $[Ru(tpy)(pydppz)]^{2+}$ and $[Ru(pydppz)_2]^{2+}$ with maxima at 698 nm ($\Phi_{em} = 2.1 \times 10^{-4}$) and 678 nm ($\Phi_{em} = 6.1 \times 10^{-4}$), respectively.[18] In contrast, the magnitude of the ^{3}MLCT luminescence quantum yield of $[Ru(tpy)(pyddpn)]^{2+}$ is ~10-fold smaller.

The E_{00} values of the ^{3}MLCT excited states of $[Ru(tpy)(pydppx)]^{2+}$, $[Ru(pydppx)_2]^{2+}$, and $[Ru(tpy)(pydppn)]^{2+}$ were estimated from the emission maxima at 77 K to be 644 (1.93 eV), 640 (1.94 eV), and 648 nm (1.91 eV), respectively. Each spectrum displays a well-defined vibronic progression with spacing of ~1280 cm^{-1} for $[Ru(tpy)(pydppx)]^{2+}$, ~1340 cm^{-1} for $[Ru(pydppx)_2]^{2+}$, and 1190 cm^{-1} for $[Ru(tpy)(pydppn)]^{2+}$, which are similar to those reported for $[Ru(tpy)_2]^{2+}$ (1290 cm^{-1}), $[Ru(tpy)(pydppz)]^{2+}$ (1312 cm^{-1}), and $[Ru(tpy)(pydppz)]^{2+}$ (1400 cm^{-1}) and can be attributed to aromatic stretching vibrations of the ligands.[18,36] Stokes shifts of 0.19 eV for $[Ru(tpy)(pydppx)]^{2+}$, 0.14 eV for $[Ru(pydppx)_2]^{2+}$, and 0.15 eV for $[Ru(tpy)(pydppn)]^{2+}$ were measured, which are typical of emissive ^{3}MLCT excited states of Ru(II) complexes.[37]

The emission lifetimes of $[Ru(tpy)(pydppx)]^{2+}$, $[Ru(pydppx)_2]^{2+}$, and $[Ru(tpy)(pydppn)]^{2+}$ range from 6.54 to 6.85 μs in ethanol/methanol (4:1 by v/v) at 77 K (Table 1) and are similar to those reported for the $[Ru(tpy)_n(pydppz)_{2-n}]^{2+}$ ($n = 0, 1$) series (~6 μs),[18] but shorter than that from the ^{3}MLCT state of $[Ru(tpy)_2]^{2+}$ (10.8 μs) at 77 K in butyronitrile (10.6 μs).[31] The measurement of the emission lifetime of the complexes was not possible at room temperature, owing to their low luminescence intensities.

Emission lifetimes of Ru polypyridine complexes typically depend on the energy gap (ΔE) between the lowest energy excited state, ^{3}MLCT, and ^{3}dd excited state(s) that undergo nonradiative deactivation.[38] This energy difference can be used to explain the significantly shorter lifetime measured for $[Ru(tpy)_2]^{2+}$ ($\tau = 250$ ps, $\Delta E \sim 1600$ cm^{-1})[39] compared to that of $[Ru(bpy)_3]^{2+}$ ($\tau = 700$ ns, ΔE ~4000 cm^{-1}).[40,41] On the basis of the E_{00} energies estimated from the emission spectra at 77 K, it is evident that the ^{3}MLCT excited states of $[Ru(tpy)(pydppx)]^{2+}$ and $[Ru(pydppx)_2]^{2+}$ lie 0.148 and 0.136 eV below that of $[Ru(tpy)_2]^{2+}$, respectively. Since the energy of the ^{3}dd state(s) among the Ru(II) tpy-type complexes is expected to be similar, the value of ΔE can be estimated to be ~2800 cm^{-1} for $[Ru(tpy)(pydppx)]^{2+}$ and ~2700 cm^{-1} for $[Ru(pydppx)_2]^{2+}$. For $[Ru(tpy)(pydppn)]^{2+}$, ΔE ~2900 cm^{-1} can be calculated from the 77 K emission maximum. The larger energy gap between the luminescent ^{3}MLCT state(s) and the nonemissive ^{3}dd state(s) in these complexes results in longer lifetimes compared to $[Ru(tpy)_3]^{2+}$ at 298 K.

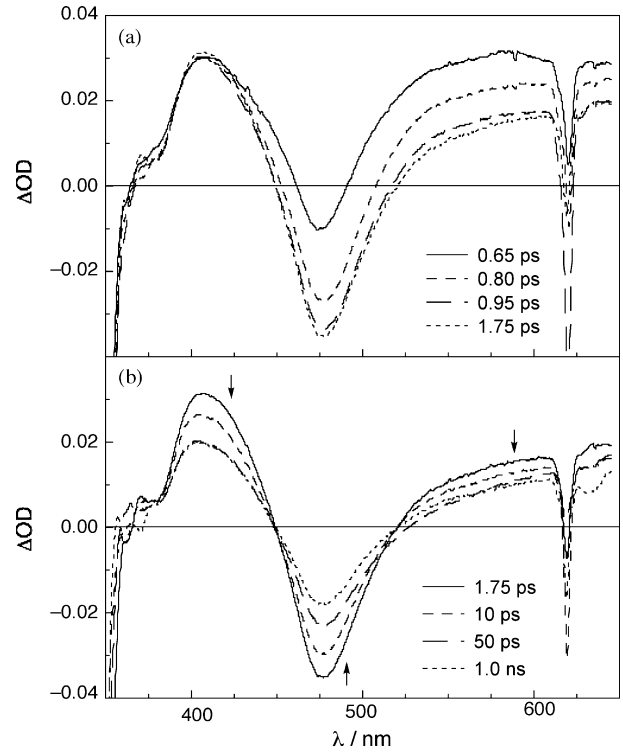

Figure 2. Transient absorption spectra of 108 μM $[Ru(tpy)(pydppx)]^{2+}$ in CH_3CN collected (a) at −1.0 to +1.75 ps and (b) +1.75 ps to +1.0 ns after the excitation pulse ($\lambda_{exc} = 310$ nm, fwhm = 300 fs).

Time-Resolved Absorption. Figures 2 and 3 show the ultrafast transient absorption spectra of $[Ru(tpy)(pydppx)]^{2+}$ and $[Ru(tpy)(pydppn)]^{2+}$ at 298 K in CH_3CN ($\lambda_{exc} = 310$ nm, fwhm ≈ 300 fs), respectively. It should be noted that the spectral features and decay kinetics of the transient absorption spectra of $[Ru(pydppx)_2]^{2+}$ and $[Ru(pydppn)_2]^{2+}$ are nearly identical to those of the corresponding heteroleptic complexes, $[Ru(tpy)(pydppx)]^{2+}$ and $[Ru(tpy)(pydppn)]^{2+}$, respectively.

The transient absorption spectra of $[Ru(tpy)(pydppx)]^{2+}$ shown in Figure 2 are characterized by strong ground-state bleaching in the 450−520 nm range and intense absorption at ~410 nm and at $\lambda > 520$ nm (CH_3CN, $\lambda_{exc} = 310$ nm, fwhm ~ 300 fs). These spectra resemble those reported for the ^{3}MLCT excited states of $[Ru(tpy)_n(pydppz)_{2-n}]^{2+}$ (n = 0−2), as well as those previously reported for tpy complexes of Ru(II) and Os(II).[42,43] Therefore, the transient absorption spectra of $[Ru(tpy)(pydppx)]^{2+}$ shown in Figure 2 are assigned to the ^{3}MLCT of the complex. The ^{3}MLCT excited state of $[Ru(tpy)(pydppx)]^{2+}$ is generated within the instrumental response time (<1 ps), followed by a fast decay with a lifetime of 17.3 ps (Figure 2a) and a slower process with $\tau = 3.7$ ns (Figure 2b). Since the spectral features of the

(36) Coe, B. J.; Thompson, D. W.; Culbertson, C. T.; Schoonover, J. R.; Meyer, T. J. *Inorg. Chem.* **1995**, *34*, 3385–95.
(37) Chen, P.; Meyer, T. J. *Chem. Rev.* **1998**, *98*, 1439–1477.
(38) Barigelletti, F.; Juris, A.; Balzani, V.; Belser, P.; Von Zelewsky, A. *J. Phys. Chem.* **1987**, *91*, 1095–8.
(39) Winkler, J. R.; Netzel, T. L.; Creutz, C.; Sutin, N. *J. Am. Chem. Soc.* **1987**, *109*, 2381–2392.
(40) Hammarstroem, L.; Barigelletti, F.; Flamigni, L.; Indelli, M. T.; Armaroli, N.; Calogero, G.; Guardigli, M.; Sour, A.; Collin, J.-P.; Sauvage, J.-P. *J. Phys. Chem. A* **1997**, *101*, 9061–9069.
(41) Juris, A.; Balzani, V.; Barigelletti, F.; Campagna, S.; Belser, P.; Von Zelewsky, A. *Coord. Chem. Rev.* **1988**, *84*, 85–277.
(42) Laine, P.; Bedioui, F.; Amouyal, E.; Albin, V.; Berruyer-Penaud, F. *Chem.—Eur. J.* **2002**, *8*, 3162–3176.
(43) (a) Collin, J. P.; Guillerez, S.; Sauvage, J. P.; Barigelletti, F.; De Cola, L.; Flamigni, L.; Balzani, V. *Inorg. Chem.* **1992**, *31*, 4112–17. (b) Sauvage, J. P.; Collin, J. P.; Chambron, J. C.; Guillerez, S.; Coudret, C.; Balzani, V.; Barigelletti, F.; De Cola, L.; Flamigni, L. *Chem. Rev.* **1994**, *94*, 993–19.

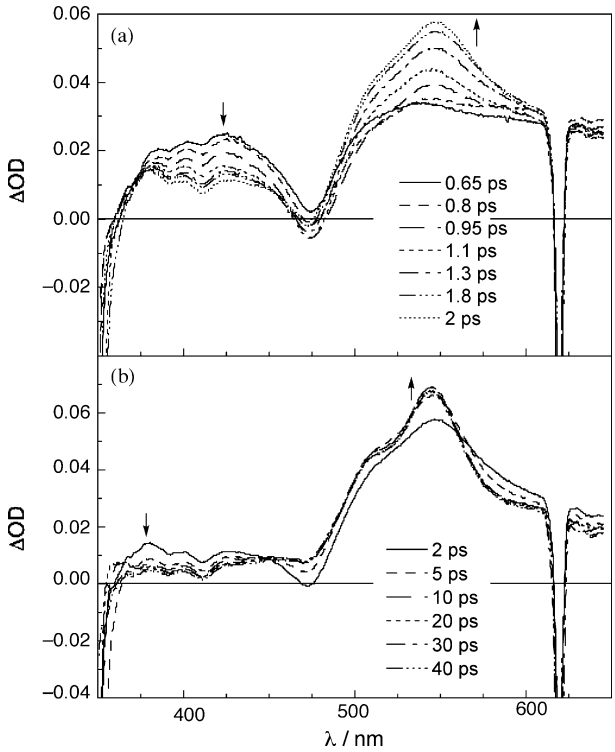

Figure 3. Transient absorption spectra of 125 μM $[Ru(tpy)(pydppn)]^{2+}$ in CH_3CN collected (a) −1.0 ps to +2.5 ps and (b) +2.5 ps to +1.0 ns after the excitation pulse (λ_{exc} = 310 nm, fwhm = 300 fs).

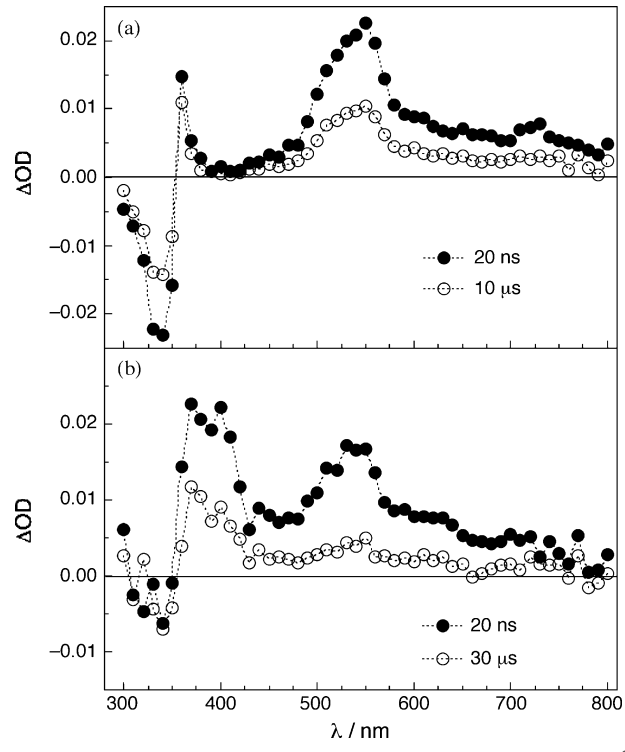

Figure 4. Transient absorption spectra of (a) 12.5 μM $[Ru(tpy)(pydppn)]^{2+}$ in CH_3CN collected 20 ns and 10 μs after the laser pulse and (b) 47 μM pydppn ligand in THF collected 20 ns and 30 μs after excitation (λ_{exc} = 355 nm, fwhm ~ 8 ns).

species generated initially are characteristic of the ^{3}MLCT excited state (which is also observed at later times), it is apparent that intersystem crossing take place in <1 ps. This observation is consistent with similar measurements on other Ru(II) and Os(II) complexes,[44−48] such as $[Ru(bpy)_3]^{2+}$, where the intersystem crossing occurs in ~40 fs.[46,47] The hot triplet manifold relaxes by vibrational cooling with τ = 17.3 ps to form the equilibrated ^{3}MLCT excited state, which exhibits a lifetime of 3.7 ns. Similarly, the lifetime of the ^{3}MLCT excited state of $[Ru(pydppx)_2]^{2+}$, 1.1 ns, is in good agreement with those of $[Ru(tpy)(pydppz)]^{2+}$ (τ = 5.4 ns), $[Ru(pydppz)_2]^{2+}$ (τ = 2.3 ns), and $[Ru(tpy)_2]^{2+}$ (τ = 0.12 ns).[18]

Figure 3 shows the transient absorption spectra of $[Ru(tpy)(pydppn)]^{2+}$ collected at various pump−probe delays in CH_3CN (λ_{exc} = 310 nm, fwhm ~ 300 fs). The spectra collected at early times (1−2 ps, Figure 3) exhibit weak absorption in the 375−450 nm range and a strong peak with a maximum at 545 nm, with superimposed features that correspond to ground state bleaching at 393, 411, and 475 nm. These spectral features are markedly different from those measured for $[Ru(tpy)_n(L)_{2-n}]^{2+}$ (L = pydppz, pydppx; n = 0−2).[18] It should be noted that the band at 545 nm is initially very broad and featureless (0.65 ps), increases in intensity to form a well-defined peak within 2 ps (Figure 3a), and then sharpens and narrows in ~22 ps (Figure 3b). Similar spectral features and kinetics were also observed for $[Ru(pydppn)_2]^{2+}$, with the band-narrowing process taking place in ~19 ps, which is interpreted as vibrational cooling.[49−51] The transient absorption spectra of $[Ru(tpy)(pydppn)]^{2+}$ and $[Ru(pydppn)_2]^{2+}$ do not exhibit any observable decay between 40 ps and 1 ns.

Figure 4a shows the transient absorption spectra of $[Ru(tpy)(pydppn)]^{2+}$ in degassed CH_3CN (λ_{exc} = 355 nm, fwhm ~8 ns) collected 20 ns and 10 μs after the laser pulse, which exhibit a strong absorption with a maximum at 545 nm and bleaching at 345 nm with τ = 20 μs. Transient absorption spectra with similar features and τ = 24 μs were obtained for $[Ru(pydppn)_2]^{2+}$ in degassed CH_3CN, and excitation of the pydppn complexes at 532 nm results in spectra with similar features and lifetimes. The excited state lifetimes of $[Ru(tpy)(pydppn)]^{2+}$ and $[Ru(pydppn)_2]^{2+}$ were measured to be 15.6 and 21.0 μs in methanol, respectively. In CH_3CN/H_2O mixtures, the lifetime of $[Ru(tpy)(pydppn)]^{2+}$ decreases linearly with the concentration of water from 18.1 μs in pure CH_3CN to 3.0 μs in H_2O. A similar dependence was measured for $[Ru(pydppn)_2]^{2+}$, from 22.6 μs in CH_3CN

(44) (a) Damrauer, N. H.; Cerullo, G.; Yeh, A.; Boussie, T. R.; Shank, C. V.; McCusker, J. K. *Science* **1997**, *275*, 54–57. (b) Yeh, A. T.; Shank, C. V.; McCusker, J. K. *Science* **2000**, *289*, 935–938.
(45) Wallin, S.; Davidsson, J.; Modin, J.; Hammarstroem, L. *J. Phys. Chem. A* **2005**, *109*, 4697–4704.
(46) Bhasikuttan, A. C.; Suzuki, M.; Nakashima, S.; Okada, T. *J. Am. Chem. Soc.* **2002**, *124*, 8398–8405.
(47) Yoon, S.; Kukura, P.; Stuart, C. M.; Mathies, R. A. *Mol. Phys.* **2006**, *104*, 1275–1282.
(48) (a) Shaw, G. B.; Papanikolas, J. M. *J. Phys. Chem. B* **2002**, *106*, 6156–6162. (b) Shaw, G. B.; Styers-Barnett, D. J.; Gannon, E. Z.; Granger, J. C.; Papanikolas, J. M. *J. Phys. Chem. A* **2004**, *108*, 4998–5006.
(49) Matousek, P.; Parker, A. W.; Towrie, M.; Toner, W. T. *J. Chem. Phys.* **1997**, *107*, 9807–9817.
(50) (a) Buntinx, G.; Naskrecki, R.; Poizat, O. *J. Phys. Chem.* **1996**, *100*, 19380–19388. (b) Buntinx, G.; Naskrecki, R.; Didierjean, C.; Poizat, O. *J. Phys. Chem. A* **1997**, *101*, 8768–8777.
(51) Iwata, K.; Hamaguchi, H.-O. *Laser Chem.* **1999**, *19*, 367–370.

to 6.4 μs in H_2O. The long lifetimes measured for these complexes are consistent with a pydppn-centered $^3\pi\pi^*$ excited state accessible following absorption into the $^1\pi\pi^*$ or ^{1}MLCT states.

In order to confirm the assignment, the nanosecond transient absorption of the free ligand, pydppn, was measured in $CHCl_3$ purged with argon (Figure 4b), which exhibits the transient absorption bands at 390 and 540 nm, and bleaching of the ground state band at 340 nm with a lifetime of 22 μs, typical of the $^3\pi\pi^*$ excited states of polycyclic aromatic heterocycles.[52] A comparison of parts a and b of Figure 4 reveals their spectral similarities, indicating that the lowest-energy excited states of $[Ru(tpy)_n(pydppn)_{2-n}]^{2+}$ ($n = 0, 1$) are localized on the pydppn ligand. Lowest energy LC $^3\pi\pi^*$ states for Ru(II) complexes, composed of covalently linked polyaromatic bidentate ligands, that exhibit a long-lived excited state were previously reported.[53−56] Lowest-energy intraligand $^3\pi\pi^*$ excited states were also reported for Ru-bpy-thiophene and Re-diimine systems, including [Re(dppz)$(CO)_3$(4-MePy)]$^+$.[57−59] For Ru(II) complexes possessing tridentate ligands with appended aromatic rings, 0.6−1.6 μs excited state lifetimes were reported, also attributed to $^3\pi\pi^*$ LC excited states.[55]

The LC $^3\pi\pi^*$ assignment is further supported by energy transfer experiments conducted with $[Ru(tpy)(pydppn)]^{2+}$ and $[Ru(pydppn)_2]^{2+}$. The transient absorption spectrum of 54 μM $[Ru(tpy)(pydppn)]^{2+}$ in CH_3CN in the presence of 30.7 μM tetracene immediately following excitation exhibits the characteristic peak for the LC $^3\pi\pi^*$ of the complex at 540 nm ($\lambda_{exc} = 532$ nm, fwhm $\sim$ 8 ns, 5 mJ/pulse), but after 10 μs, new absorption bands at 390 and 460 nm appear, which are in good agreement with the known spectrum of the $^3\pi\pi^*$ excited state of tetracene.[60,61] It should be noted that tetracene does not absorb light at 532 nm; therefore, formation of its $^3\pi\pi^*$ must be sensitized by the $[Ru(tpy)(pydppn)]^{2+}$ complex. The rate constants of triplet−triplet energy transfer, k_{EnT}, were measured using Stern−Volmer kinetics for $[Ru(tpy)(pydppn)]^{2+}$ and $[Ru(pydppn)_2]^{2+}$ with a number of organic systems with varying $^3\pi\pi^*$ energies, listed in Table 2.[62] It is evident from Table 2 that the values of k_{EnT} decrease sharply when the energy of the $^3\pi\pi^*$ excited state of the acceptor, $E(^3\pi\pi^*)$, is greater than $\sim$1.5 eV for both complexes. Therefore, the LC $^3\pi\pi^*$ excited states of $[Ru(tpy)(pydppn)]^{2+}$ and $[Ru(pydppn)_2]^{2+}$ are estimated to lie $\sim$1.5 eV above the ground state. This value is consistent with the energy of the phosphorescence measured at 77 K for the free pydppn ligand in an ethanol/methanol (v/v, 4:1) glass.

Table 2. Energy Transfer Quenching Rate Constants for $[Ru(tpy)(pydppn)]^{2+}$ and $[Ru(pydppn)_2]^{2+a}$

Acceptor	$E(^3\pi\pi^*)$/eV[b]	k_{EnT}/M^{-1} s^{-1} $[Ru(tpy)(pydppn)]^{2+}$	k_{EnT}/M^{-1} s^{-1} $[Ru(pydppn)_2]^{2+}$
tetracene	1.27	4.4×10^9	2.4×10^9
perylene	1.53	3.5×10^9	2.6×10^9
9,10-diBr-anthracene	1.74	6.1×10^6	2.5×10^6
phenazine	1.93	3.2×10^6	2.2×10^6

[a] CH_3CN, 298 K. [b] From ref 62.

Excited State Manifolds. A generalized Jablonski diagram for $[Ru(tpy)(pydppx)]^{2+}$ and $[Ru(pydppx)_2]^{2+}$ is shown in Figure 5a using measured or estimated energies of the various excited states. The E_{00} energies of the ^{3}MLCT states were determined to be 1.93 for $[Ru(tpy)(pydppx)]^{2+}$ and 1.94 eV for $[Ru(pydppx)_2]^{2+}$ from the emission maxima at 77 K, while the energies of the ^{1}MLCT states were estimated from the ground state absorption spectra to be 2.26 and 2.59 eV, respectively. Similarly, the absorption spectra led to pydppx $^1\pi\pi^*$ energies of 3.22 eV for both complexes. The energies of the LC $^3\pi\pi^*$ excited states of $[Ru(tpy)(pydppx)]^{2+}$ and $[Ru(pydppx)_2]^{2+}$ were estimated to be $\sim$2.25 eV from the phosphorescence of the free pydppx ligand at 77 K in an ethanol/methanol (v/v, 4:1) glass. The LF ^{3}dd state(s) are expected to lie at an energy similar to that in $[Ru(tpy)_2]^{2+}$, estimated at 2.29 eV.[39] In these complexes, the LC $^3\pi\pi^*$ lies above the ^{3}MLCT state, which is typical for Ru(II) complexes, including $[Ru(tpy)_2]^{2+}$, $[Ru(tpy)(pydppz)]^{2+}$, and $[Ru(pydppz)_2]^{2+}$. In Figure 5a, direct excitation from the ^{1}GS (ground state) to the ^{1}MLCT or LC $^1\pi\pi^*$ states results in intersystem crossing to generate the lowest energy ^{3}MLCT excited state within 1 ps. The initially produced hot ^{3}MLCT state of each complex vibrationally cools within $\sim$20 ps, then decays to the ^{1}GS in the nanosecond time scale.

The energies of the ^{1}MLCT excited states of $[Ru(tpy)(pydppn)]^{2+}$ and $[Ru(pydppn)_2]^{2+}$ were estimated at 2.62 and 2.60 eV, respectively, and in both complexes, the $^1\pi\pi^*$ and ^{3}dd excited states are predicted at 2.99 and 2.29 eV, respectively. The energy of the ^{3}MLCT state of $[Ru(tpy)(pydppn)]^{2+}$ was estimated at 1.91 eV from the 77 K emission, and the same value was used for $[Ru(pydppn)_2]^{2+}$, since no emission was observed for the latter. In the pydppn complexes, the $^3\pi\pi^*$ state, at $\sim$1.5 eV, lies $\sim$0.4 eV below the corresponding ^{3}MLCT state, making the former the lowest energy excited state in these systems. A generalized

(52) (a) Carmichael, I.; Hug, G. L. *J. Phys. Chem. Ref. Data* **1986**, *15*, 1–250. (b) Carmichael, I.; Helman, W. P.; Hug, G. L. *J. Phys. Chem. Ref. Data* **1987**, *16*, 239–60.
(53) McClenaghan, N. D.; Leydet, Y.; Maubert, B.; Indelli, M. T.; Campagna, S. *Coord. Chem. Rev.* **2005**, *249*, 1336–1350.
(54) Hissler, M.; Harriman, A.; Khatyr, A.; Ziessel, R. *Chem.—Eur. J.* **1999**, *5*, 3366–3381.
(55) Ding, H.-Y.; Wang, X.-S.; Song, L.-Q.; Chen, J.-R.; Yu, J.-H.; Chao, L.; Zhang, B.-W. *J. Photochem. Photobiol. A* **2006**, *177*, 286–294.
(56) (a) Goeb, S.; De Nicola, A.; Ziessel, R.; Sabatini, C.; Barbieri, A.; Barigelletti, F. *Inorg. Chem.* **2006**, *45*, 1173–1183. (b) Goze, C.; Sabatini, C.; Barbieri, A.; Barigelletti, F.; Ziessel, R. *Inorg. Chem.* **2007**, *46*, 7341–7350.
(57) (a) Harriman, A.; Mayeux, A.; De Nicola, A.; Ziessel, R. *Phys. Chem. Chem. Phys.* **2002**, *4*, 2229–2235. (b) De Nicola, A.; Liu, Y.; Schanze, K. S.; Ziessel, R. *Chem. Commun.* **2003**, 288–289. (c) Liu, Y.; De Nicola, A.; Reiff, O.; Ziessel, R.; Schanze, K. S. *J. Phys. Chem. A* **2003**, *107*, 3476–3485. (d) Harriman, A.; Khatyr, A.; Ziessel, R. *Dalton Trans.* **2003**, 2061–2068.
(58) (a) Goze, C.; Kozlov, D. V.; Tyson, D. S.; Ziessel, R.; Castellano, F. N. *New J. Chem.* **2003**, *27*, 1679–1683. (b) Kozlov, D. V.; Tyson, D. S.; Goze, C.; Ziessel, R.; Castellano, F. N. *Inorg. Chem.* **2004**, *43*, 6083–6092.
(59) Stoeffler, H. D.; Thornton, N. B.; Temkin, S. L.; Schanze, K. S. *J. Am. Chem. Soc.* **1995**, *117*, 7119–28.
(60) Pavlopoulos, T. G. *J. Chem. Phys.* **1972**, *56*, 227–32.
(61) Meyer, Y. H.; Astier, R.; Leclercq, J. M. *J. Chem. Phys.* **1972**, *56*, 801–15.
(62) Murov, S. L. *Handbook of Photochemistry*; Marcel Dekker Inc.: New York, 1973.

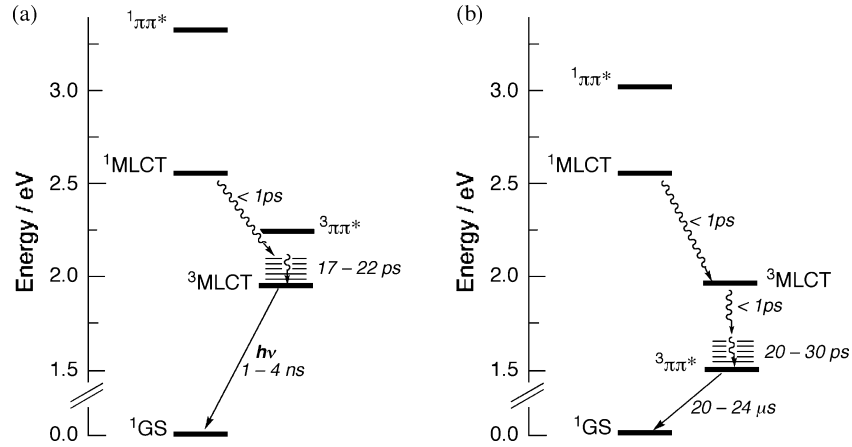

Figure 5. Generalized Jablonski diagrams for (a) $[Ru(tpy)_n(pydppx)_{2-n}]^{2+}$ ($n = 0$, 1) and (b) $[Ru(tpy)_n(pydppn)_{2-n}]^{2+}$ ($n = 0$, 1).

Jablonski diagram is shown in Figure 5b for these complexes. Although the LC $^3\pi\pi^*$ excited state affords the microsecond lifetimes of the excited $[Ru(tpy)(pydppn)]^{2+}$ and $[Ru(pydppn)_2]^{2+}$ complexes, the ultrafast measurements are consistent with the population of the ^{3}MLCT excited state at early times. These results indicate that there is mixing of the ^{3}MLCT and $^3\pi\pi^*$ manifolds in the initially generated hot triplet state, which relaxes to the $^3\pi\pi^*$ after vibrational cooling.

Sensitized Production of $^1O_2$. Owing to the long lifetimes and energies of the $^3\pi\pi^*$ excited states of $[Ru(tpy)(pydppn)]^{2+}$ and $[Ru(pydppn)_2]^{2+}$, it is expected that they should be able to sensitize the production of $^1O_2$ in high yields. The quantum yields of photosensitized production of $^1O_2$ by $[Ru(tpy)_n(L)_{2-n}]^{2+}$ (L = pydppx, pydppn; $n = 0$, 1) were measured using $[Ru(bpy)_3]^{2+}$ as a standard ($\Phi_{^1O_2} = 0.81$ in CH_3OH)[63] and 1,3-diphenyl-isobenzofuran as a trapping agent for the detection of $^1O_2$.[64] Indeed, the values of $\Phi_{^1O_2}$ for $[Ru(tpy)(pydppn)]^{2+}$ and $[Ru(pydppn)_2]^{2+}$ were measured to be 0.92(2) and 1.07(7), respectively, in CH_3OH ($\lambda_{irr} = 475$ nm). In contrast, the short lifetimes of the ^{3}MLCT excited states of $[Ru(tpy)(pydppx)]^{2+}$ and $[Ru(pydppx)_2]^{2+}$ led to very low production of $^1O_2$ upon irradiation, with quantum yields of 0.014(3) and 0.010(4), respectively. As expected, the measured quantum yields of the photogeneration of $^1O_2$ follow the lifetimes of the excited states, which increase in the order $[Ru(pydppx)_2]^{2+}$ (1.1 ns) < $[Ru(tpy)(pydppx)]^{2+}$ (3.7 ns) ≪ $[Ru(tpy)(pydppn)]^{2+}$ (20.1 μs) < $[Ru(pydppn)_2]^{2+}$ (24.3 μs) in CH_3OH.

For $[Ru(tpy)(pydppn)]^{2+}$ and $[Ru(pydppn)_2]^{2+}$, the quantum yields of $^1O_2$ photosensitization are close to unity. To our knowledge, these bis-tridentate Ru(II) complexes represent the most efficient $^1O_2$ photosensitizers of their class reported to date. In addition, these values exceed those reported for the currently used PDT drug Photofrin, composed of hematoporphyrin and its derivatives, for which $\Phi_{^1O_2} = 0.75$ was reported in ethanol.[65] The higher sensitization yield by these Ru(II) complexes stems from the presence of the heavy metal, which makes the intersystem crossing to the triplet manifold nearly unity. Therefore, these systems may be potentially useful as PDT agents. As an initial survey of their possible usefulness, the binding and photocleavage of the complexes to DNA was measured.

DNA Binding and Photocleavage. The changes in the electronic absorption spectra of $[Ru(tpy)_n(pydppn)_{2-n}]^{2+}$ ($n = 0$, 1) and $[Ru(tpy)(pydppx)]^{2+}$ as a function of DNA concentration were used to estimate the DNA binding constant, K_b, of each complex (5 mM Tris buffer, pH = 7.5, 50 mM NaCl) using a typical DNA binding model (see the Supporting Information).[18,27,28] The absorption spectrum of 8.9 μM $[Ru(tpy)(pydppn)]^{2+}$ exhibits hypochromic shifts of 33% (328 nm) and 23% (474 nm) in the presence of 62.9 μM DNA, and a modest bathochromic shift of ~3 nm (5 mM Tris, pH = 7.5, 50 mM NaCl), resulting in $K_b = 4.6 \times 10^6$ M^{-1} ($s = 1.34$). Similarly, 35% (385 nm) and 21% (474 nm) hypochromicities were measured for 8.6 μM $[Ru(tpy)(pydppx)]^{2+}$ upon the addition of up to 63 μM DNA, from which $K_b = 6.9 \times 10^5$ M^{-1} ($s = 1.32$) was determined from the fit. The absorption changes resulted in $K_b = 3.5 \times 10^5$ M^{-1} ($s = 0.56$) for 10.5 μM $[Ru(pydppn)_2]^{2+}$ upon the addition of up to 67 μM DNA, along with hypochromicities of 20% (350 nm) and 12% (385 nm). For $[Ru(pydppx)_2]^{2+}$, the addition of small concentrations of DNA resulted in an increase in absorption, followed by a decrease in intensity. This behavior has been previously correlated with solution aggregation of the probe, such that determination of the DNA binding constant cannot be calculated using the present model.[15,29,66,67] The DNA binding constants measured for $[Ru(tpy)_n(pydppn)_{2-n}]^{2+}$ ($n = 0$, 1) and $[Ru(tpy)(pydppx)]^{2+}$ are similar to those reported for other intercalating molecules and related Ru(II) complexes, such as ethidium bromide (1.7×10^5 M^{-1}),[68] $[Ru(tpy)(pydppz)]^{2+}$ (2×10^6 M^{-1}),[18] $[Ru(phen)_2(dppz)]^{2+}$ ($1-5 \times 10^6$ M^{-1}; phen = 1,10-phenanthroline),[69,70] and $[Ru(bpy)_2(tpphz)]^{2+}$ (5.1×10^6

(63) Bhattacharyya, K.; Das, P. K. *Chem. Phys. Lett.* **1985**, *116*, 326–32.
(64) Young, R. H.; Wehrly, K.; Martin, R. L. *J. Am. Chem. Soc.* **1971**, *93*, 5774–9.
(65) Dougherty, T. J.; Gomer, C. J.; Weishaupt, K. R. *Cancer Res.* **1976**, *36*, 2330–3.
(66) (a) Angeles-Boza, A. M.; Bradley, P. M.; Fu, P. K.-L.; Shatruk, M.; Hilfiger, M. G.; Dunbar, K. R.; Turro, C. *Inorg. Chem.* **2005**, *44*, 7262. (b) Chouai, A.; Wicke, S.; Turro, C.; Bacsa, J.; Dunbar, K. R.; Thummel, R. P. *Inorg. Chem.* **2005**, *44*, 5996.
(67) Liu, Y.; Chouai, A.; Degtyareva, N. N.; Lutterman, D. A.; Dunbar, K. R.; Turro, C. *J. Am. Chem. Soc.* **2005**, *127*, 10796–10797.
(68) (a) Tang, T.-C.; Huang, H.-J. *Electroanalysis* **1999**, *11*, 1185. (b) Paoletti, C.; Le Pecq, J. B.; Lehman, I. R. *J. Mol. Biol.* **1971**, *55*, 75.

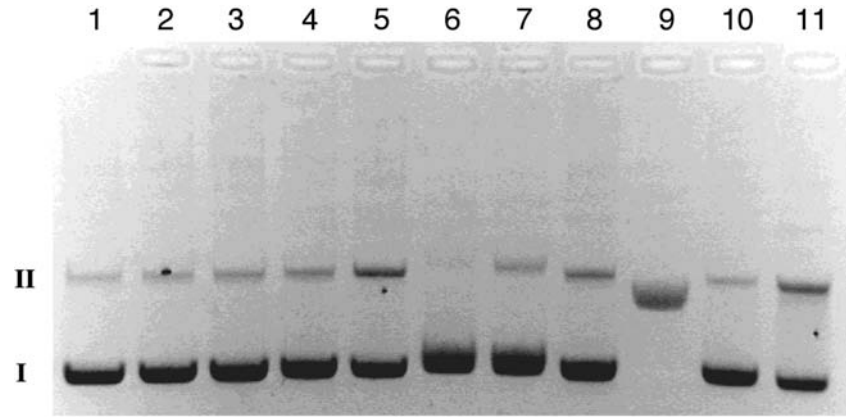

Figure 6. Ethidium bromide stained agarose gel (2%) of 75 μM pUC18 plasmid, showing the photocleavage by Ru(II) complexes (15 μM) in the air (5 mM Tris, 50 mM NaCl, pH = 7.5). Lane 1, plasmid only; lanes 2 and 3, $[Ru(tpy)_2]^{2+}$; lanes 4 and 5, $[Ru(tpy)(pydppx)]^{2+}$; lanes 6 and 7, $[Ru(pydppx)_2]^{2+}$; lanes 8 and 9, $[Ru(tpy)(pydppn)]^{2+}$; lanes 10 and 11, $[Ru(pydppn)_2]^{2+}$. Lanes 1, 2, 4, 6, 8, and 10: dark. Lanes 3, 5, 7, 9, and 11: irradiated with $\lambda_{irr} > 395$ nm (10 min).

M^{-1}).[67] The lower K_b value measured for $[Ru(tpy)(pydppx)]^{2+}$ compared to the pydppn complexes may be due to steric hindrance provided by the two methyl groups in the former. Similar results were recently reported for $[Ru(bpy)_2(dppx)]^{2+}$ (dppx = 11,12-dimethyl-dipyrido[3,2-*a*:2′,3′-*c*]phenazine) compared to $[Ru(bpy)_2(dppz)]^{2+}$.[71]

The lifetime of the $^3\pi\pi^*$ excited state of 13.9 μM $[Ru(tpy)(pydppn)]^{2+}$ increases from 2.65 μs in deaereated buffer (5 mM Tris, pH = 7.5, 50 mM NaCl) to 13.1 μs in the presence of 146 μM DNA. The lifetime of the transient absorption of $[Ru(tpy)(pydppn)]^{2+}$ and its spectral features observed when the complex is bound to DNA are similar to those in CH_3CN. Unlike $[Ru(phen)_2(dppz)]^{2+}$, where 0.5 M H_2O in CH_3CN quenches the emission from the complex, the behavior observed for $[Ru(tpy)(pydppn)]^{2+}$ parallels that of $[(dppz)Re(CO)_3(4\text{-}MePy)]^+$, for which the lowest energy excited state is $^3\pi\pi^*$ with a long lifetime in H_2O.[59] Similar results were observed for $[Ru(pydppn)_2]^{2+}$, with a lifetime of 13.3 μs when bound to DNA.

Figure 6 shows the DNA photocleavage by $[Ru(tpy)_2]^{2+}$ and for $[Ru(tpy)_n(L)_{2-n}]^{2+}$ (L = pydppx, pydppn; $n = 0, 1$) upon irradiation ($\lambda_{irr} > 395$ nm, 10 min). pUC18 plasmid alone appears in lane 1 as a control (Figure 6), where the major fraction of the sample is in the supercoiled form (form I) with a small amount of nicked plasmid (form II). Although the DNA photocleavage by $[Ru(tpy)_2]^{2+}$ and $[Ru(tpy)_n(pydppz)_{2-n}]^{2+}$ ($n = 0, 1$) was previously shown to be mediated by $^1O_2$, the amount of cleavage was very small owing to the short lifetime of the excited state.[18] Similar results are observed here for $[Ru(tpy)(pydppx)]^{2+}$ (lane 5) and $[Ru(pydppx)_2]^{2+}$ (lane 7), which do not exhibit significant DNA photocleavage under these conditions. Lane 11 shows the photocleavage by $Ru(pydppn)_2]^{2+}$, showing a greater amount of nicked DNA (form II) formed compared to the dark control (lane 10). The efficiency of DNA photocleavage is significantly greater for $[Ru(tpy)(pydppn)]^{2+}$, where lane 9 shows the complete disappearance of the undamaged plasmid (form I) and the formation of a broad, weaker band at a position between those of forms I and II. Although the product of double-strand breaks, linearized form (form III), typically appears between form I and form II, in this case, the broadening and lower intensity from the ethidium bromide stain is consistent with numerous single-strand breaks to the same plasmid (Figure S6, Supporting Information). It should be pointed out that none of the complexes cleave DNA in the dark or when the experiments are conducted under a deoxygenated atmosphere (Figure S7, Supporting Information). In addition, greater photocleavage is observed for $[Ru(tpy)(pydppn)]^{2+}$ when the experiment is conducted in D_2O (Figure S7, Supporting Information), consistent with the longer lifetime of $^1O_2$ in D_2O compared to that in H_2O.[72] The long excited state lifetimes of $[Ru(tpy)(pydppn)]^{2+}$ and $[Ru(pydppn)_2]^{2+}$ and the dependence of the photocleavage of these complexes on the presence of oxygen, along with greater photocleavage in D_2O, point at DNA damage mediated by sensitized $^1O_2$. The greater DNA photocleavage by $[Ru(tpy)(pydppn)]^{2+}$ compared to $[Ru(pydppn)_2]^{2+}$ can be attributed to the ~10-fold greater value of K_b of the former. The mechanism operative in the DNA photocleavage reaction remains unknown at this time and is a point of current investigation.

Conclusions

Ru(II) complexes possessing the tridentate ligands tpy, pydppx, and pydppn, $[Ru(tpy)_n(L)_{2-n}]^{2+}$ (L = pydppx, pydppn, $n = 0-2$), were synthesized, and their steady-state and time-resolved photophysical properties were investigated. The Ru(II) complexes possessing the pydppx ligand are similar to the pydppz systems, with a lowest energy ^{3}MLCT excited state with lifetimes of 1−4 ns. In contrast, the lowest energy excited state in the $[Ru(tpy)_n(pydppn)_{2-n}]^{2+}$ ($n = 0$, 1) complexes is a LC $^3\pi\pi^*$ localized on the pydppn ligand with lifetimes of ~20 μs. The $[Ru(tpy)_n(pydppn)_{2-n}]^{2+}$ ($n = 0, 1$) complexes are able to generate $^1O_2$ with quantum

(69) Haq, I.; Lincoln, P.; Suh, D.; Norden, B.; Chowdhry, B. Z.; Chaires, J. B. *J. Am. Chem. Soc.* **1995**, *117*, 4788–96.
(70) Nair, R. B.; Teng, E. S.; Kirkland, S. L.; Murphy, C. J. *Inorg. Chem.* **1998**, *37*, 139–141.
(71) Sun, Y.; Lutterman, D. A.; Turro, C. *Inorg. Chem.* **2008**, *47*, 6427–6434.
(72) (a) Merkel, P. B.; Kearns, D. R. *J. Am. Chem. Soc.* **1972**, *94*, 1029–1030. (b) Merkel, P. B.; Nilsson, R.; Kearns, D. R. *J. Am. Chem. Soc.* **1972**, *94*, 1030–1031.

yields of ~100%, which leads to its efficient mediation of DNA photocleavage for $[Ru(tpy)(pydppn)]^{2+}$, owing to its greater DNA binding constant. Such high quantum yields of $^1O_2$ photosensitization may be useful in the design of new metal complexes with long-lived excited states for PDT.

Acknowledgment. C.T. thanks the National Science Foundation (CHE 0503666) and The Center for Chemical and Biophysical Dynamics (CCBD) at the Ohio State University for their generous support. D.A.L. thanks the OSU for a University Presidential Graduate Fellowship. R.P.T. thanks the Robert A. Welch Foundation (E-621) and the National Science Foundation (CHE-0352617) for financial support. The authors also thank Dr. G. Burdzinski and Dr. T. Takaya for their help tuning for the fs laser.

Supporting Information Available: DNA binding model and titrations, DNA photocleavage gels in D_2O and irradiation time dependence. This material is available free of charge via the Internet at http://pubs.acs.org.

IC801636U